

Parameterizing the Geometry of the QGP on an Event-by-Event Basis

Ben Bert¹, Coleridge Faraday¹ and W.A. Horowitz^{1,2}

¹Department of Physics, University of Cape Town, 7701 Rondebosch, South Africa

²Department of Physics, New Mexico State University, Las Cruces, New Mexico, 88003, USA

E-mail: ben.bert.1303@gmail.com

Abstract. Ultra-relativistic heavy-ion collisions create a nuclear fireball that serves as a powerful laboratory for probing the frontiers of Quantum Chromodynamics (QCD). In recent years, there has been growing interest in the study of small collision systems—such as proton-proton (pp) and proton-nucleus (pA)—at facilities like RHIC and the LHC. Many of the assumptions underlying the energy loss formalism developed in the Djordjevic-Gyulassy-Levai-Vitev (DGLV) model, break down in these small systems. In this work, we present an extension of the energy loss model developed by Faraday and Horowitz (FH) which itself is an extension of the DGLV formalism that specifically accounts for the unique features of small system dynamics. This is achieved by relaxing the large formation time approximation and introducing an additional correction term that accounts for short path lengths in the medium. By relaxing these assumptions, one encounters a more intricate analytic structure for the energy loss, and thus increased computational demands; we address this challenge by developing a novel numerical scheme. Our approach accurately parametrizes the geometry of the quark-gluon plasma (QGP), resulting in a dramatic computational speedup—improving efficiency by up to seven orders of magnitude.

1 Introduction

The nuclear modification factor (R_{AA}) is a key observable for studying the energy loss of high transverse momentum (p_T) particles traversing the Quark-Gluon Plasma (QGP). Rooted in Bjorken’s jet quenching framework, the R_{AA} quantifies the suppression of particle yields in heavy-ion collisions relative to proton-proton systems [1]. Experiments at RHIC observed a suppression in light hadron spectra by a factor of five, signaling strong partonic energy loss in the QGP [2].

More recently, signatures of QGP formation—including quarkonium suppression, strangeness enhancement, and collective flow—have also been identified in small collision systems—such as pp and pA —at RHIC and the LHC [3]. However, small systems pose unique challenges, such as centrality bias, which arises from correlations between soft and hard particles [4].

Azimuthal anisotropies in detected spectra, as quantified by the v_n flow coefficients, offer further insights into the properties of the QGP, including transport properties and the path-length-dependent energy loss of partons [5, 6].

The azimuthal anisotropies can be characterized through a Fourier decomposition of the observed spectra, the Fourier decompositions are given in terms of the v_n Fourier coefficients and the event plane angle ψ_n . Due to detector acceptance effects and finite particle multiplicity, the measured event plane angles fluctuate event-by-event around the true event plane angles. To account for these fluctuations, *resolution factors* are introduced to correct the measured v_n coefficients; the resolution factors however, induce an ambiguity into the measured v_n coefficients [7]. The *scalar product* method of measuring the v_n coefficients, couples soft and hard hadrons in a

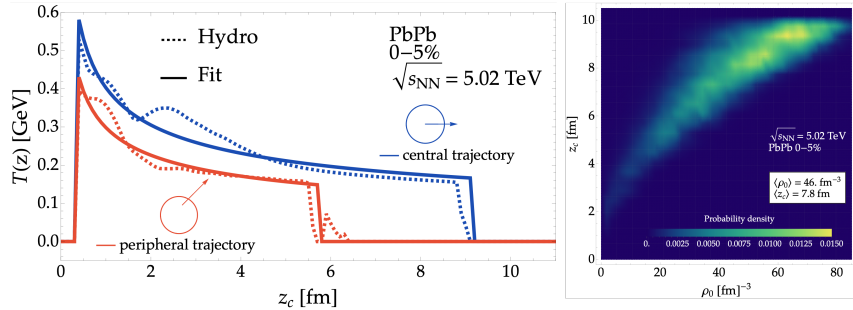


Figure 1: (Left): Comparison of temperature distributions obtained from hydrodynamic simulations (dotted curves) and the corresponding fitted temperature distribution (solid curves) for two paths through the medium. The red curves have initial positions of $x_0 = (1.5, 4.5)$ fm and angles $\phi = \pi/4$, and are representative of characteristic *peripheral* trajectories; the blue curves have initial positions of $x_0 = (0, 0)$ fm and angles $\phi = 0$, and are representative of characteristic *central* trajectories. The hydrodynamic temperature distribution comes from a PbPb 0–5% collision system at $\sqrt{s_{NN}} = 5.02$ TeV. For the peripheral trajectory, $z_c = 5.7$ fm and $\rho_0 = 30.5 \text{ fm}^{-3}$; for the central trajectory, $z_c = 9.1$ fm and $\rho_0 = 74.9 \text{ fm}^{-3}$. (Right): Correlation between ρ_0 and z_c parameters for 0–5% PbPb collision system at $\sqrt{s_{NN}} = 5.02$ TeV. The first moments for the $P_{geo}(\rho_0, z_c)$ distribution (with the angular dependency integrated out) are found for this collision system to be $\langle \rho_0 \rangle = 46.0 \text{ fm}^{-3}$ and $\langle z_c \rangle = 7.8 \text{ fm}$.

given centrality while avoiding the ambiguities induced by the resolution factors and is thus considered to be a more robust measurement of the v_n coefficients [8, 9].

It has proven to be a challenge on theoretical grounds to simultaneously predict the R_{AA} and the v_n coefficients—a tension known as the $R_{AA} \otimes v_n$ puzzle. One of the contributions known to effect the tension is attributed to the omission of soft-sector fluctuations and event-by-event fluctuations of the initial state [5].

In this work we use the energy loss model developed by Faraday and Horowitz (FH) which has extended the DGLV radiative energy loss formalism by including short path-length corrections and collisional energy loss using Hard Thermal Loop (HTL) kinematics [10]. Their model adopts a static, brick-like medium and parameterizes the scattering center using an effective path length [10, 11, 12, 13, 14].

The primary focus of this manuscript will be to develop a framework that describes the nuclear modification factor while simultaneously describing the anisotropic flow harmonics. We extend upon the work of FH by including event-by-event fluctuations of the bulk geometry and relaxing the brick-like and static simplification of the bulk’s geometry.

2 Parametrization of Trajectories

The energy loss of a parton in the QGP depends on its path and the medium’s geometry. As calculating energy loss for all possible trajectories can be computationally expensive (see section 2.2 for a more in depth discussion), we follow the previous work of [10, 11] by mapping each trajectory to two parameters—which the energy loss can be made to be dependent on—the energy loss can then be averaged over these parameters to capture the global effects of the collision system.

We model the energy loss in terms of a scattering center density $\bar{\rho}$, which is related to the medium density ρ via $\rho = (N_s/A_\perp)\bar{\rho}$, where N_s is the number of scatterings, A_\perp the transverse area of the medium. The medium density ρ can be expressed in terms of the medium’s temperature through elementary thermodynamic relations as $\rho = 4\zeta(3)(4+n_f)T^3/(\pi^2)$. To model ρ along each trajectory, we fit the medium density with power-law profile as $\rho_{fit}(z) = \rho_0(\tau_0/z)^{1.2} \theta(z_c - z)\theta(z - \tau_0)$, with the formation time of the medium $\tau_0 = 0.4$ fm. The choice of τ_0 is made as this is the turn-on time for the hydrodynamics simulations we use [15]. The corresponding fitted temperature profile is then $T_{fit}(z) = (\pi^2 \rho_{fit}(z)/4\zeta(3)(4+n_f))^{1/3}$. For each path, the cutoff z_c is determined by the distance at which the hydrodynamic temperature distribution drops below the thermalization temperature, and ρ_0 is fixed by ensuring that the area under the temperature curve is the same for both the hydrodynamic temperature profile (obtained from the IP-Glasma model [15]) and the fitted temperature profile. In fig. 1 (Left) we show a comparison of the hydrodynamic temperature distribution and the fitted temperature distribution for two characteristic paths through the medium.

To generalize to an entire event ensemble, we define a probability distribution over (ρ_0, z_c) for a fixed angle ϕ through the medium by assuming that the initial parton production scales with n_{coll} , the number of binary

collisions density. In fig. 1 (Right) we show the correlation between the ρ_0 and z_c parameters for a PbPb 0–5% collision system at $\sqrt{s_{NN}} = 5.02$ TeV.

2.1 Energy Loss

In this work, we model the energy loss of a parton moving through the QGP by taking into account radiative and elastic contributions. Following FH [10, 12, 13, 14] we use the WHDG [11] formalism along with its short path length correction [16] to model the radiative sector of the energy loss, and we model the elastic energy loss by using an effective field theory called Hard Thermal Loops (HTL). Our implementation of the energy loss relaxes the static brick assumption used by FH; the formalism we make use of allows the Debye mass μ and gluon mass m_g to depend on the temperature of the medium at each point of the parton's trajectory through the medium.

2.2 Numerical challenges of the energy loss

Conceptually, the most simple method of calculating the energy loss on a path-by-path basis would be to compute the energy loss using the true hydrodynamic temperature profile and then using the expression for ρ to find the associated medium density. To capture the global effects, one would then simply average over all the different paths through the medium. However, the total number of paths one would need to consider to resolve the QGP would typically involve ~ 20 angles and a grid of size $\sim 15 \times 15$ (fm)² with intervals of ~ 0.05 (fm). To capture the event-by-event fluctuations, one would need to calculate the energy loss another $\sim 10^3$ times, one for each event. Note that the parameters specified here are estimates of the typical resolution used in model, but the specific values will vary depending on the collision system.

This computational expensiveness is why we introduce the ρ_0 and z_c parameters, as these parameters allow us to calculate the energy loss as a function of the two parameters and then use a distribution of the ρ_0 and z_c parameters (see the right panel of fig. 1) to capture the global effects. The entire phase space of possible paths requires a grid of ρ_0 and z_c parameters such that $\rho_0 \in [1, 100]$ fm⁻³ and $z_c \in [0.4, 11]$ fm with intervals of 10 fm⁻³ and 1 fm respectively. Thus, calculating the energy loss by using the fitted parameter method proves to be seven orders of magnitude faster than more direct method described in the preceding paragraph. Note that the evaluating the energy loss in terms of the fitted parameters closely resembles the energy loss calculation done if we were to use the true hydrodynamic temperature profile; this good agreement between the two methods validates the use of the fitted parameter method.

3 Observables

3.1 Nuclear Modification Factor

The nuclear modification factor of a parton q in an $A + A$ collision system is defined as

$$R_{AA}^q(p_T, \phi) \equiv \frac{d^2 N_{AA,f}^q / dp_T d\phi}{N_{coll} d^2 N_{pp,f}^q / dp_T d\phi} = \int \frac{dx}{1-x} P_{tot}(x|\phi) \frac{f_{AA}^q\left(\frac{p_T}{1-x}, \phi\right)}{f_{pp}^q(p_T, \phi)} \quad (1)$$

where $d^2 N_{AA,f}^q / dp_T d\phi$ and $d^2 N_{pp,f}^q / dp_T d\phi$ are the parton spectra in $A + A$ and $p + p$ collisions after interactions with the medium respectively; N_{coll} is the average number of binary collisions, typically calculated using the Glauber model [17]. The second equality in eq. (1) grants us access to the R_{AA} on theoretical grounds, and is true if one assumes the following: (1) The partonic spectrum of the initial state in a $p + p$ collision, scales like the partonic spectrum of the initial state in an $A + A$ collision, weighted by $1/N_{coll}$. (2) All modifications to the $A + A$ differential spectrum arises from the energy loss through interactions with the medium. (3) The proton-proton spectrum is unmodified by the medium. Note that we have defined the notational device $f_{pp/AA}^q(p_T, \phi)$ as:

$$f_{pp}^q(p_T, \phi) \equiv \frac{d^2 N_{pp,i}^q}{dp_T d\phi} \quad \& \quad f_{AA}^q(p_T, \phi) \equiv \frac{1}{N_{coll}} \frac{d^2 N_{AA,i}^q}{dp_T d\phi} \quad (2)$$

where in eq. (2), the i subscript is used to denote the spectrum of the initial state.

3.2 Azimuthal Anisotropies

The observed azimuthal anisotropy in high- p_T hadrons allows for the study of the energy loss and the path length dependence of hard partons moving though the QGP [5]. In this work, an analogue to the $v_n\{SP\}$ coefficients measured experimentally is developed from a theoretical point of view (see section 3.4). This is done so that the theory predictions made in our study are more comparable to what is being observed experimentally. As part of the framework developed here, we incorporate event-by-event fluctuations of the initial state into the calculation of the v_n and $v_n\{SP\}$ coefficients. In fig. 2 we demonstrate that accounting for these fluctuations is crucial for addressing the $R_{AA} \otimes v_2$ puzzle.

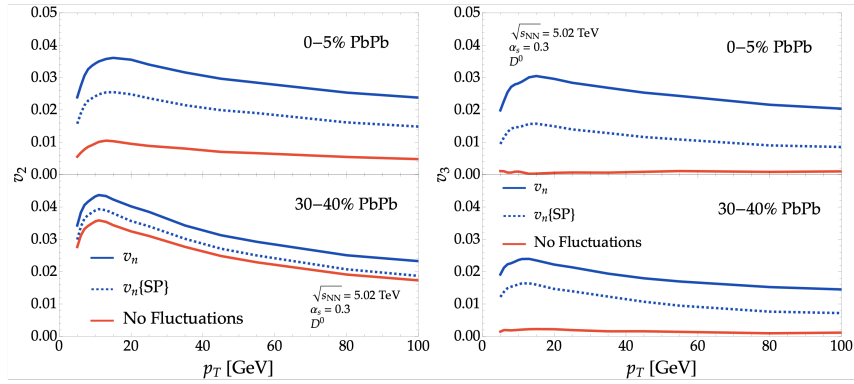


Figure 2: (Left): Comparison of Fourier, Scalar Product v_2 and the Fourier v_2 without fluctuations as a function of p_T for D^0 mesons. The event-by-event fluctuations are turned off by evaluating eq. (5) with R_{AA} averaged over all events instead of event-by-event R_{AA} . All curves are calculated with the strong coupling fixed at $\alpha_s = 0.3$. The top (bottom) panel shows the results where the geometric average is calculated over a PbPb 0-5% (30-40%) centrality collision system. (Right): The same as (Left) but for v_3 instead of v_2 .

3.3 Azimuthal Anisotropies from Fourier Expansions

The azimuthal anisotropy in the distributions of the observed final state hadrons can be characterized by a Fourier expansion [7]

$$\frac{2\pi}{N_{AA,f}^{h,k}} \frac{dN_{AA,f}^{h,k}}{d\phi} = \frac{R_{AA}^{h,k}(p_T, \phi)}{R_{AA}^{h,k}(p_T)} = 1 + 2 \sum_{n=1}^{\infty} v_n^k \cos(n[\phi - \psi_n^k]) \quad (3)$$

where the v_n^k coefficients are the uniquely determined Fourier coefficients, ψ_n^k are the event plane angles, and the k index specifies a particular event.

3.4 Scalar Product v_n

The scalar product (SP) method of determining the reaction plane experimentally is achieved through the use of \vec{Q}_n flow vectors. The \vec{Q}_n vectors provide an approximation to the reaction plane and are determined from the final state particles via [7]

$$\mathcal{Q}_n \equiv Q_n e^{in\Psi_n} = \sum_j e^{in\phi_j}, \quad (4)$$

One may then take the real and imaginary parts of \mathcal{Q}_n to be the x and y component of the \vec{Q}_n vector respectively. To access the \vec{Q}_n in our energy loss formalism, we make use of the IP-Glasma model which is then evolved with the MUSIC viscous relativistic (2 + 1) D hydrodynamics code, followed by UrQMD microscopic hadronic transport [15]. The j index in eq. (4) is summed over final state particles from all oversampled UrQMD simulations and the azimuthal angle is $\phi_j = \arctan 2(p_j^y, p_j^x)$. The $v_n\{SP\}$ coefficients are defined here as

$$v_n\{SP\} \equiv \frac{\langle \vec{u}_n \cdot \vec{Q}_n \rangle}{\sqrt{\langle Q_n^2 \rangle}} = \sum_{k=1}^{N_e} \frac{\int_0^{2\pi} d\phi R_{AA}^{h,k}(p_T, \phi) \vec{Q}_n^k \cdot \vec{u}_n^k(\phi)}{2\pi \sqrt{\langle Q_n^2 \rangle} N_e R_{AA}^{h,k}(p_T)} \quad (5)$$

in line with what is commonly done experimentally [8, 9]. In eq. (5) the vector \vec{u}_n is defined as $\vec{u}_n \equiv (\cos n\phi, \sin n\phi)$, where ϕ is the azimuthal direction of the hadronic candidate. The quantity $\langle \vec{u}_n \cdot \vec{Q}_n \rangle$ in eq. (5), is an average over all events and over different \vec{u}_n vectors associated with the observed hadrons; $\langle Q_n^2 \rangle$ is only averaged over the events. The second equality in eq. (5) provides us access to the $v_n\{SP\}$ coefficient on theoretical grounds, and follows from the first equality in eq. (5) if one assumes that the distribution of initial hard jet production is proportional to the number of binary collision density $n_{coll}^k(\vec{x})$.

4 Results

In this section we present our model's predictions for the R_{AA} and v_2 coefficients. All comparisons to data are made with the strong coupling α_s varied between 0.25 and 0.3. Note that we only present results for large system data (PbPb) as calculations for small systems are yet to be complete.

In fig. 3 we show the prediction of the model for charged particles in PbPb collisions at 0-5% and 30-40% centrality for both the R_{AA} and the v_2 . The R_{AA} data is from the CMS [18] and ATLAS [19] experiments respectively; the v_2 data comes from the same collaborations [8, 9].

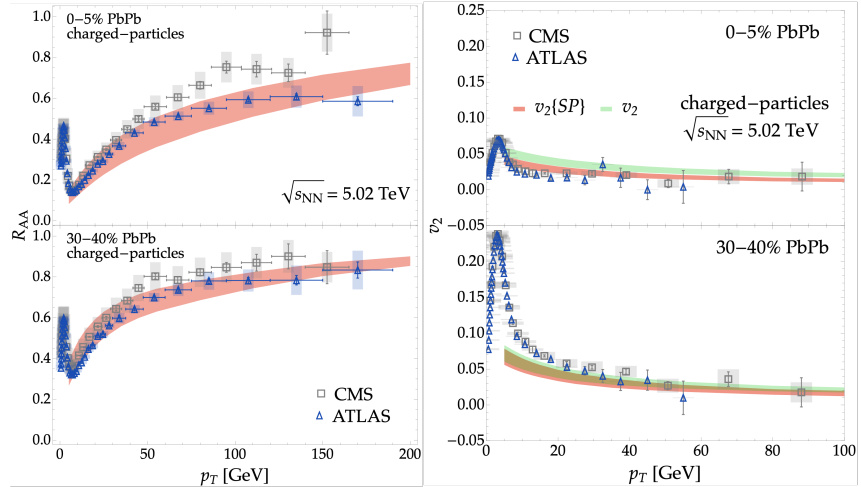


Figure 3: (Left): Comparison of R_{AA} predictions to CMS [18] and ATLAS [19] data for charged particles in 0-5% (top) and 30-40% (bottom) PbPb. (Right): v_2 predictions for charged particles vs CMS/ATLAS in 0-5% (top) and 30-40% (bottom) PbPb [8, 9].

5 Conclusions and Outlook

In this manuscript, we presented a modification to the formalism developed by FH [10, 12, 13, 14], in which the static brick assumption has been relaxed. The model we present here takes into account the temperature profile of the medium as a function of the parton's path through said medium; the dynamic nature of the temperature on a path-by-path basis is captured by parametrizing a power law dependency (through ρ_{fit}) of the medium density through two fitted parameters. The energy loss of a parton moving through the medium can be calculated in terms of these two fitted parameters, this leads to a dramatic numerical speed up—which is vitally important for statistically robust modeling of event-by-event fluctuations.

For high- p_T charged particles, the model is in good agreement with v_2 data for PbPb collisions systems and shows the correct qualitative centrality dependence as the model's predictions for the v_2 increase as the collisions become more peripheral. The same conclusions can be drawn for the models predictive capabilities when comparing to the R_{AA} of high- p_T charged particles in PbPb collision systems.

Future work will focus on completing the model's predictions for small collision systems by performing a χ^2 minimization to find the optimal value of α_s which best describes both the R_{AA} and v_2 data in large systems, and then using this extracted value of α_s to make predictions for small systems, as done in [14]. As the initial state effects are thought to be more pronounced in small systems, another route of future work will be to perform an analysis of the effects of the initial temperature dependence (*i.e.* before the formation time τ_0) on the energy loss and the associated observables. Furthermore, the effects of our choice of parameterization of the medium density is to be compared to the results obtained when using the true hydrodynamic temperature profile on a path-by-path basis is planned for future work.

Acknowledgements

The authors would like to thank the South African National Research Foundation (NRF), the National Institute for Theoretical and Computational Sciences (NITheCS), and the SA-CERN collaboration.

References

- [1] J. D. Bjorken, “Energy loss of energetic partons in quark-gluon plasma: Possible extinction of high p_t jets in hadron-hadron collisions,” Fermilab, Tech. Rep. FERMILAB-PUB-82-059-THY, 1982, unpublished.
- [2] K. Adcox *et al.*, “Suppression of hadrons with large transverse momentum in central Au+Au collisions at $\sqrt{s_{NN}} = 130$ -GeV,” *Phys. Rev. Lett.*, vol. 88, p. 022301, 2002.

- [3] J. F. Grosse-Oetringhaus and U. A. Wiedemann, “A Decade of Collectivity in Small Systems,” Jul. 2024, arXiv:2407.07484 [hep-ex].
- [4] J. Adam *et al.*, “Centrality dependence of particle production in p-Pb collisions at $\sqrt{s_{NN}} = 5.02$ TeV,” *Phys. Rev. C*, vol. 91, no. 6, p. 064905, 2015.
- [5] J. Noronha-Hostler, B. Betz, J. Noronha, and M. Gyulassy, “Event-by-event hydrodynamics + jet energy loss: A solution to the $R_{AA} \otimes v_2$ puzzle,” *Phys. Rev. Lett.*, vol. 116, no. 25, p. 252301, 2016.
- [6] M. Aaboud *et al.*, “Measurement of the suppression and azimuthal anisotropy of muons from heavy-flavor decays in Pb+Pb collisions at $\sqrt{s_{NN}} = 2.76$ TeV with the ATLAS detector,” *Phys. Rev. C*, vol. 98, no. 4, p. 044905, 2018.
- [7] M. Luzum and J.-Y. Ollitrault, “Eliminating experimental bias in anisotropic-flow measurements of high-energy nuclear collisions,” *Phys. Rev. C*, vol. 87, no. 4, p. 044907, 2013.
- [8] M. Aaboud *et al.*, “Measurement of the azimuthal anisotropy of charged particles produced in $\sqrt{s_{NN}} = 5.02$ TeV Pb+Pb collisions with the ATLAS detector,” *Eur. Phys. J. C*, vol. 78, no. 12, p. 997, 2018.
- [9] A. M. Sirunyan *et al.*, “Azimuthal anisotropy of charged particles with transverse momentum up to 100 GeV/ c in PbPb collisions at $\sqrt{s_{NN}} = 5.02$ TeV,” *Phys. Lett. B*, vol. 776, pp. 195–216, 2018.
- [10] C. Faraday, A. Grindrod, and W. A. Horowitz, “Inconsistencies in, and short pathlength correction to, $R_{AA}(p_T)$ in A + A and p + A collisions,” *Eur. Phys. J. C*, vol. 83, no. 11, p. 1060, 2023.
- [11] S. Wicks, W. Horowitz, M. Djordjevic, and M. Gyulassy, “Elastic, inelastic, and path length fluctuations in jet tomography,” *Nucl. Phys. A*, vol. 784, pp. 426–442, 2007.
- [12] C. Faraday and W. A. Horowitz, “Collisional and radiative energy loss in small systems,” *Phys. Rev. C*, vol. 111, no. 5, p. 054911, 2025.
- [13] ———, “A unified description of small, peripheral, and large system suppression data from pQCD,” *Phys. Lett. B*, vol. 864, p. 139437, 2025.
- [14] ———, “Statistical analysis of pQCD energy loss across system size, flavor, $\sqrt{s_{NN}}$, and p_T ,” May 2025, arXiv:2505.14568 [hep-ph].
- [15] B. Schenke, C. Shen, and P. Tribedy, “Running the gamut of high energy nuclear collisions,” *Phys. Rev. C*, vol. 102, no. 4, p. 044905, 2020.
- [16] I. Kolbe and W. A. Horowitz, “Short path length corrections to Djordjevic-Gyulassy-Levai-Vitev energy loss,” *Phys. Rev. C*, vol. 100, no. 2, p. 024913, 2019.
- [17] M. L. Miller, K. Reygers, S. J. Sanders, and P. Steinberg, “Glauber modeling in high energy nuclear collisions,” *Ann. Rev. Nucl. Part. Sci.*, vol. 57, pp. 205–243, 2007.
- [18] V. Khachatryan *et al.*, “Charged-particle nuclear modification factors in PbPb and pPb collisions at $\sqrt{s_{NN}} = 5.02$ TeV,” *JHEP*, vol. 04, p. 039, 2017.
- [19] G. Aad *et al.*, “Charged-hadron production in pp, p+Pb, Pb+Pb, and Xe+Xe collisions at $\sqrt{s_{NN}} = 5$ TeV with the ATLAS detector at the LHC,” *JHEP*, vol. 07, p. 074, 2023.